Katabatic flow with Coriolis effect and gradually varying eddy diffusivity

Iva Kavčič · Branko Grisogono

Abstract Katabatic flows over high-latitude long glaciers experience the Coriolis force. A sloped atmospheric boundary-layer (ABL) flow is addressed which partly diffuses upwards, and hence, becomes progressively less local. We present the analytical and numerical solutions for (U, V, θ) depending on (z, t) in the katabatic flow, where U and V are the downslope and cross-slope wind components and θ is the potential temperature perturbation. A Prandtl model that accounts for the Coriolis effect, via f, does not approach a steady state, because V diffuses upwards in time; the rest, i.e., (U, θ), are similar to that in the classic Prandtl model. The V component behaves in a similar manner as the solution to the 1st Stokes (but inhomogeneous) problem. A WKB approach to the problem of the sloped ABL winds is outlined in the light of a modified Ekman-Prandtl model with gradually varying eddy diffusivity $K(z)$. Ideas for parameterizing these high-latitude persistent flows in climate models are revealed.

Keywords Low-level jet · Prandtl model · Strongly stable boundary layer

1 Introduction

Katabatic flows are regular features of the stable atmospheric boundary layer (ABL) over inclined radiatively cooled surfaces. The ubiquitous nature of katabatic flows over e.g., Antarctica and Greenland, not to mention smaller areas such as Iceland,

After Wentzel, Kramers and Brillouin, who popularized the method in theoretical physics.

I. Kavčič(✉)
Department of Geophysics, Faculty of Science, University of Zagreb, Horvatovac bb, 10 000 Zagreb, Croatia
e-mail: ivakavc@gfz.hr

B. Grisogono
Department of Geophysics, Faculty of Science, University of Zagreb, Zagreb, Croatia

Atmospheric Boundary Layers. A. Baklanov & B. Grisogono (eds.),
doi: 10.1007/978-0-387-74321-9_15,

and their cumulative effects, implies that the katabatic wind contributes to the general circulation (Parish and Bromwich 1991). Moreover, as katabatic flows may impinge on various coasts (Parmhed et al. 2004; Renfrew and Anderson 2006; Söderberg and Parmhed 2006), they may interact with sea ice and coastal ocean areas. It has been considered that katabatic flows might affect the thermohaline circulation and water mass conversions through the formation of coastal polynyas and the associated strong air–sea interaction (e.g., Gordon and Comiso 1988).

The detailed structure of katabatic flow still remains an important modelling issue (e.g., Weng and Taylor 2003). The stably stratified boundary layer is usually poorly resolved in many numerical models (e.g., Zilitinkevich et al. 2006), i.e., the modelling of katabatic flows is reasonably successful only if a sufficient vertical resolution is used (e.g., Renfrew 2004). A simple model of katabatic flows represents a balance between the negative buoyancy production due to the surface potential temperature deficit and dissipation by turbulent fluxes (e.g., Mahrt 1982; Egger 1990). On long glaciers in higher latitudes the Coriolis force also becomes an important contributor to the katabatic flow balance, deflecting the downslope component and leading to the occurrence of a wind component directed across the slope (Denby 1999; Van den Broeke et al. 2002). Stiperski et al. (2007) extended the Prandtl model by including the Coriolis force in order to be able to cover long polar slopes and the corresponding long-lived strongly stable ABL.

Furthermore, the pure katabatic flow is characterized by a pronounced low-level jet (LLJ) and sharp near-surface vertical temperature gradient (e.g., King et al. 2001; Grisogono and Oerlemans 2001a,b; Van den Broeke et al. 2002). Renfrew (2004) and Renfrew and Anderson (2006) show that significant katabatic flows over Antarctica most often exhibit clearly their LLJ and an anticlockwise backing of the wind with height. The authors suggest that this is due to a decrease in frictional forcing with height through the ABL. Moreover, Renfrew and Anderson (2006) indicate which kind of problems the measurements of katabatic flows may have, e.g., capturing the height of the LLJ that may exist just above a meteorological mast but still below the lowest sodar level. These authors illustrate that even a fine-scale nonhydrostatic numerical weather prediction (NWP) model encounters problems in modelling these widespread flows (to capture the jet-shaped shallow flow a model set-up with high vertical resolution is required), not to mention typical course-grid climate models. Therefore, katabatic flows typically have to be parameterized in large-scale models (e.g., Zilitinkevich et al. 2006), and to this end we further develop the Prandtl model with the Coriolis effect and variable eddy diffusivity.

King et al. (2001) show how sensitive the modelled Antarctic climate is to modifications of ABL parameterizations. Ever increasing resolution of the NWP and various regional models calls for continuous and necessary improvements of current parameterizations (e.g., various corrections to the Obukhov length). There is hardly any horizontal surface over land where the NWP model grid spacing falls below several km; in fact, slopes are typically between 0.5° and 10° to 20°. The surface slope, aside from violating horizontal homogeneity assumption, affects also Monin–Obukhov (MO) scaling as such: MO theory considers only the vertical component of the buoyancy (e.g., Munro and Davies 1978), neglecting its role as the driving force for katabatic flow in the horizontal momentum equation. In this study we revoke a known suggestion that an additional alternative for surface-layer scaling may be invoked — that from the Prandtl model relating to the LLJ height (Munro 1989, 2004; Grisogono and Oerlemans 2001a,b).

We continue the work of Grisogono and Oerlemans (2001a,b) by introducing a gradually varying eddy diffusivity in the analytical model given in Stiperski et al. (2007). The new approximate (and possibly asymptotic) solutions for katabatic boundary-layer flows, obtained by using e.g., the WKB method, may be useful in explaining various measurements (e.g., over the Antarctic), and to lend credibility for a more faithful parameterization of katabatic flows in meteorological and climate models. The paper is organized as follows. In Sect. 2 we present the main findings of Stiperski et al. (2007) as a starting point for introducing the varying eddy diffusivity. In Sect. 3 numerical solutions and approximate WKB solutions are presented. The conclusions are given in Sect. 4.

2 Rotating Prandtl model and solutions for constant eddy diffusivity

The rotating Prandtl model describes a hydrostatic, one-dimensional Boussinesq flow with the effects of the Coriolis force included. As in the classical Prandtl model (Mahrt 1982; Egger 1990; Parmhed et al. 2004), the K-theory is invoked to model the turbulent fluxes. The governing equations of the rotating model are thoroughly derived in Stiperski et al. (2007) under the assumption of a constant eddy thermal diffusivity K_c and a constant turbulent Prandtl number Pr. In the case of non-constant K, the equations for the downslope and cross-slope components of the wind vector (U, V), the potential temperature perturbation θ (total minus the background prescribed potential temperature) and the corresponding boundary conditions are:

$$\frac{\partial U}{\partial t} = g\frac{\theta}{\theta_0}\sin(\alpha) + f\cos(\alpha)V + \mathrm{Pr}\,\frac{\partial}{\partial z}\left(K\frac{\partial U}{\partial z}\right), \tag{1}$$

$$\frac{\partial V}{\partial t} = -f\cos(\alpha)U + \mathrm{Pr}\,\frac{\partial}{\partial z}\left(K\frac{\partial V}{\partial z}\right), \tag{2}$$

$$\frac{\partial \theta}{\partial t} = -\gamma\sin(\alpha)U + \frac{\partial}{\partial z}\left(K\frac{\partial \theta}{\partial z}\right), \tag{3}$$

$$\theta(z=0) = C, U(z=0) = V(z=0) = 0, \tag{4}$$

$$\theta(z\to\infty) = U(z\to\infty) = V(z\to\infty) = 0. \tag{5}$$

Here the z axis is not vertical but perpendicular to the surface (x axis) sloped with the negative (clockwise) angle α from the horizontal. The symbols have their usual meaning: θ_0 is a reference potential temperature, f is the Coriolis parameter, g is acceleration due to gravity and $C < 0$ is the constant surface-potential-temperature deficit, applied to an undisturbed atmosphere–surface interface instantaneously at the time $t = 0$. Slope angle α, for which the katabatic wind is successfully treated by the model, typically does not exceed 10°, therefore giving a reasonable assumption of using the constant gradient of the background potential temperature γ in the true vertical (Eq. 3). More about the model derivation can be found in e.g., Denby (1999).

Equations (1) through (5) can be used to describe the "primarily katabatic driven" flow, as selected by the criteria described in Renfrew and Anderson (2002). That is, such flows develop in the stable ABL where the surface radiation balance is a net cooling to space and the mesoscale pressure gradient is small, so that the influence from larger-scale weather systems is reduced. Such "typical" katabatic flow is shal-

low, with winds aloft decaying with height and rather weak compared to near-surface winds (Renfrew and Anderson 2006).

Before attempting to derive the analytical solutions for U, V and θ let us briefly revisit the main conclusions of Stiperski et al. (2007) for the case of $K(z) = K_c$, as they represent the starting point of discussion for the more general case of varying K.

- The approximate solutions for the steady-state potential temperature perturbation and down-slope velocity component (θ_s and U_s) are analogous to the classical Prandtl model:

$$\theta_s = C \exp\left(-\frac{z}{h_p}\right) \cos\left(\frac{z}{h_p}\right), \tag{6}$$

$$U_s = \frac{C K_c \sigma^2}{\gamma \sin(\alpha)} \exp\left(-\frac{z}{h_p}\right) \sin\left(\frac{z}{h_p}\right), \tag{7}$$

where $h_p = \sqrt{2}/\sigma$ is the Prandtl layer height,

$$\sigma = \left(\frac{N^2 \,\mathrm{Pr} \sin^2(\alpha) + f^2 \cos^2(\alpha)}{\mathrm{Pr}^2 K_c^2}\right)^{1/4}, \tag{8}$$

and N is the buoyancy (Brunt-Vaisala) frequency, satisfying $N^2 = \gamma g/\theta_0$. In (6) and (7) θ_s and U_s are the solutions of the 6th-order partial differential equation for each of the unknowns represented by the flow vector $F = (\theta, U, V)$:

$$\frac{\mathrm{d}^2}{\mathrm{d}z^2}\left(\frac{\mathrm{d}^4 F}{\mathrm{d}z^4} + \sigma^4 F\right) = 0. \tag{9}$$

Numerical solutions for U and θ asymptotically approach their steady state values U_s and θ_s after the characteristic time scale for the katabatic flow $T = 2\pi/(N sin(\alpha))$ (Mahrt 1982; Grisogono 2003).

- Numerical solution for the cross-slope velocity component does not reach the steady state, but diffuses upwards through a several hundred m thick layer. However, the scale analysis carried out in Stiperski et al. (2007) has shown that the changes in V do not exert a significant influence on U and θ, which remain very close to their steady profiles U_s and θ_s. The ratio of the Coriolis term to the buoyancy term in (1) is, for typical katabatic flows, $\mathrm{O}(10^{-2})$; hence, it is reasonable to neglect the Coriolis term for the analytical treatment of the simplified problem. Then (1) and (3) become weakly decoupled from (2), which becomes a forced diffusion equation. The analytic solution for V is thus obtained from Eq. (2), with U_s on the right-hand side as its forcing:

$$V_f = \frac{Cf \cot(\alpha)}{\mathrm{Pr}\,\gamma}\left[1 - erf\left(\frac{z}{2\sqrt{tK_c\,\mathrm{Pr}}}\right) - \exp\left(-\frac{z}{h_p}\right)\cos\left(\frac{z}{h_p}\right)\right]. \tag{10}$$

The above solution holds after time $t > T$ needed for the forcing in (2), via U_s, to approach its steady state.

The derived solutions, together with the results from Grisogono (2003), lead us to the hypothesis that similar behaviour can also be expected in the case of a vertically varying eddy diffusivity. That is, the numerical results for U and θ would approach steady state within $T - 1.5T$, while V would continue to diffuse upwards, only this time with the limitations imposed by the $K(z)$ profile. Thus, V would behave as a solution to the 1st Stokes inhomogeneous problem (e.g., Kundu and Cohen 2002).

3 Solutions for varying eddy diffusivity

3.1 The WKB solutions

For $K = K(z)$, analytical solutions can be derived using the WKB method (Grisogono 1995; Grisogono and Oerlemans 2001a,b). More about the mathematical background of the method can be found in Bender and Orszag (1978). Furthermore, its use for pure katabatic flows is justified in Grisogono and Oerlemans (2002) and Parmhed et al. (2004).

We apply the method with a zero-order solution for θ and U. This approach keeps the balance between the terms with the largest amplitude in Eq. (9), modified for the varying K. Here, the derivatives of K are neglected and only its variations in σ are allowed. Nevertheless, it must be emphasized that, for the WKB method to be valid, the $K(z)$ profile must be either constant or gradually varying with respect to the vertical scale variations of the analytical solution. The latter means not only that $K(z)$ has to be a gradually varying function itself (Grisogono and Oerlemans 2001a), but also that the height of the maximum value of $K(z)$ (hereafter denoted by $K_{\max}$) must be above the LLJ height. In this paper we use the analytical $K(z)$ profile from Grisogono and Oerlemans (2001a,b), and Parmhed et al. (2004):

$$K(z) = K_{\max}\sqrt{e}\frac{z}{h}\exp\left(-\frac{z^2}{2h^2}\right), \tag{11a}$$

$$K_{\max} = 3K_c, \tag{11b}$$

where h is the level where $K_{\max}$ is reached. Here h can be estimated from the fact that the WKB solution for U will always place the LLJ below that calculated via the constant-K solution (Grisogono and Oerlemans 2001a,b). Moreover, the position of the LLJ height in V_f is always higher than in U_s, and also gradually increases in time, reaching $\approx 100\,\mathrm{m}$ (Stiperski et al. 2007). Simultaneously, the value of h is limited by the depth of the strongly stable ABL (Grisogono and Oerlemans 2002). The above conditions, together with the conditions imposed by the WKB method, give us a reasonable estimate of $h = 200\,\mathrm{m}$ for the $K(z)$ profile used in the following example (Subsect. 3.2).

Relations between the best choices for K_c and $K_{\max}$ are discussed in Grisogono and Oerlemans (2001a). Here we just adopt the fact that it is reasonable if $K_c \approx 30\%$ of $K_{\max}$, as in Eq. (11b). Of course, other choices are possible depending on specific cases addressed. Further details on estimating $K_{\max}$ and h can be found in Grisogono and Oerlemans (2002) and Parmhed et al. (2004); Parmhed et al. (2005).

As discussed in Sect. 2, following the scale analysis in Stiperski et al. (2007) we neglect the Coriolis term in (1). This enables us to straightforwardly use the zero-order WKB approach for the modified flow vector $F = (\theta, U)$:

$$F_0 \propto \exp\left[-\frac{(1-i)}{\sqrt{2}}\sigma_0 I(z)\right], \tag{12}$$

where

$$I(z) = \int_0^z K(z)^{-1/2}\,\mathrm{d}z, \tag{13}$$

and

$$\sigma_0^4 = \frac{N^2 \,\mathrm{Pr} \sin^2(\alpha) + f^2 \cos^2(\alpha)}{\mathrm{Pr}^2}. \tag{14}$$

Furthermore, we define:

$$\sigma_{\mathrm{WKB}}(z) = \sigma_0 I(z), \tag{15}$$

which, together with the boundary conditions given in Eqs. (4) and (5), yield the solutions for θ and U:

$$\theta_{\mathrm{WKB}} = C \exp\left(-\frac{\sigma_{\mathrm{WKB}}(z)}{\sqrt{2}}\right) \cos\left(\frac{\sigma_{\mathrm{WKB}}(z)}{\sqrt{2}}\right), \tag{16}$$

$$U_{\mathrm{WKB}} = \frac{C\sigma_0^2}{\gamma \sin(\alpha)} \exp\left(-\frac{\sigma_{\mathrm{WKB}}(z)}{\sqrt{2}}\right) \sin\left(\frac{\sigma_{\mathrm{WKB}}(z)}{\sqrt{2}}\right). \tag{17}$$

As can be seen from previous studies (Grisogono 1995; Grisogono and Oerlemans 2001a,b, 2002) the WKB solutions are structurally similar to the constant-K case. In this study $I(z)$ is evaluated numerically, but it may be calculated also analytically, carefully taking into consideration its often divergent nature that is successfully overcome by the negative exponential in (12), and then in (16) and (17).

Moreover, the WKB solutions approach the constant-K solutions (6) and (7) as $K(z) \to K_c$. Then, $I(z)$ in (13) becomes $K_c^{-1/2} z$, and $\sigma_{\mathrm{WKB}}(z)/\sqrt{2}$ in (16) and (17) becomes $\sigma z/\sqrt{2} = z/h_p$ (Eqs. 6 and 7). This yields a reasonable assumption that V_f may also be considered as the limit value of the corresponding WKB solution and implies the expansion of the argument of the error function in (10) for the case of variable $K(z)$. That is, $zK_c^{-1/2} \to I(z)$ in (10), giving us the solution for $V(z,t)$:

$$V_{\mathrm{WKB}} \approx \frac{Cf \cot(\alpha)}{\mathrm{Pr}\,\gamma} \left[1 - erf\left(\frac{I(z)}{2\sqrt{t\,\mathrm{Pr}}}\right) - \exp\left(-\frac{\sigma_{\mathrm{WKB}}(z)}{\sqrt{2}}\right) \cos\left(\frac{\sigma_{\mathrm{WKB}}(z)}{\sqrt{2}}\right)\right]. \tag{18}$$

Again, $t > T$ as in (10). The comparison between the analytical and numerical solutions, as well as comparison with the constant-K case, is given in the following section.

3.2 Comparison with the numerical and constant-K solutions

Following Stiperski et al. (2007), the analytical solutions are verified against the numerical solutions of the time-dependent system (1)–(3) obtained using the simple numerical model from Grisogono (2003). The numerical and WKB solutions for U and $\theta^{\mathrm{tot}} = \theta + \gamma z$ are compared for a case with physical parameters $(f, \alpha, \gamma, Pr, C) = (1.1 \times 10^{-4}\,\mathrm{s}^{-1}, -4°, 4 \times 10^{-3}\,\mathrm{K\,m}^{-1}, 1.1, -8°\mathrm{C})$, and the prescribed $K(z)$ from (11a) and (11b). Here θ^{tot} is calculated and plotted without the reference potential temperature θ_0 (to reword, the constant θ_0 is already subtracted from θ^{tot}). From Fig. 1 it can be seen that the numerical solution (dashed) for both U and θ^{tot} are in excellent agreement with the steady state solutions (16) and (17) for $t \geq T$ (solid). Such agreement is expected from the results for the constant-K case described in Stiperski et al. (2007, see their Figure 2).

Figure 2 displays both the WKB and constant-K solutions for U and θ^{tot}, showing the improvement in describing the sharp near-surface gradients in temperature

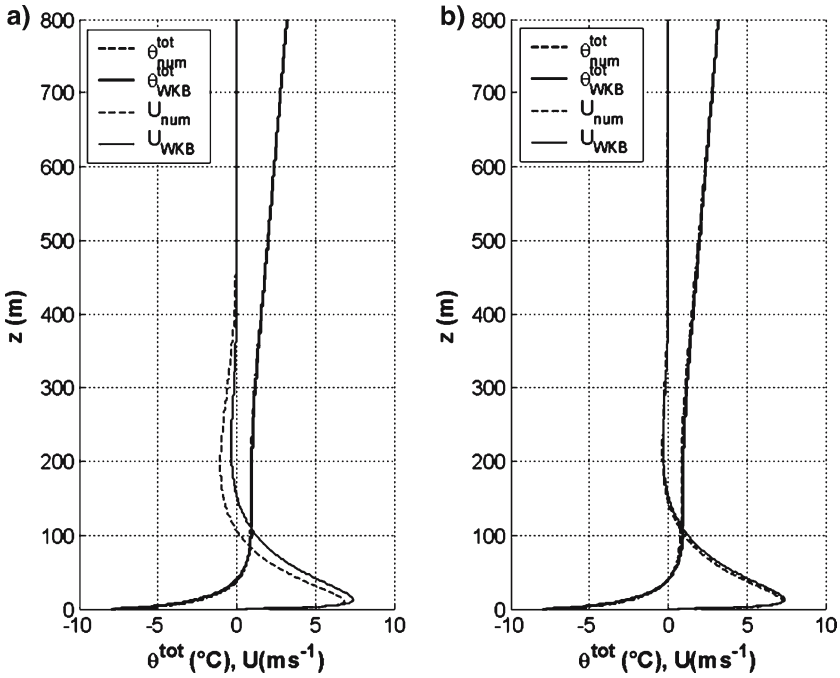

Fig. 1 Numerical $\theta^{\rm tot}_{\rm num}$ and $U_{\rm num}$ (dashed) and analytical WKB $\theta^{\rm tot}_{\rm WKB}$ and $U_{\rm WKB}$ (solid), Eqs. (16) and (17), solutions for the Prandtl model, at (**a**) $t = T$ and (**b**) $t = 10T$, $T = 2\pi/(N\sin(\alpha)) \approx 2.1$ h. Here $K(z)$ is from (11a) and (11b), with $K_{\max} = 3\,{\rm m^2 s^{-1}}$ at $h = 200$ m; other parameters are $(f, \alpha, \gamma, Pr, C) = (1.1 \times 10^{-4}\,{\rm s^{-1}}, -4°, 4 \times 10^{-3}\,{\rm K\,m^{-1}}, 1.1, -8°{\rm C})$. The numerical model top is at 2,000 m

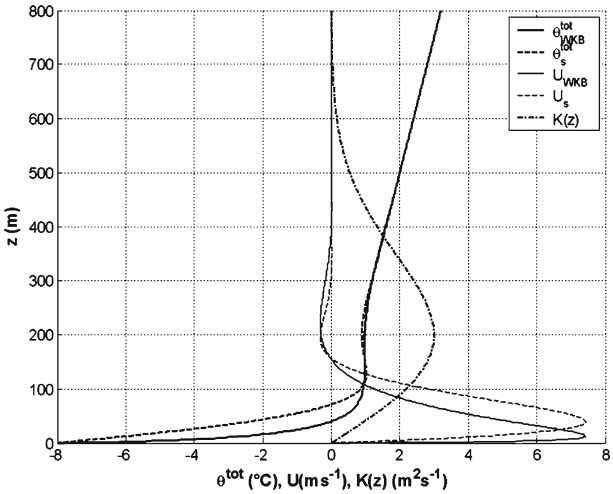

Fig. 2 The prescribed $K(z)$ profile (dot-dashed) and analytic solutions of the rotating Prandtl model for the case of varying (solid) and constant K (dashed). Here $K(z)$ is from Eqs. (11a) and (11b), $K_c = 1\,{\rm m^2 s^{-1}}$, and $\theta^{\rm tot}_s$ and U_s from (6) and (7). The rest as in Fig. 1

and wind that are often observed (Defant 1949; Munro 1989; Egger 1990; Oerlemans 1998; Parmhed et al. 2004). This is also in agreement with the analysis of Grisogono and Oerlemans (2001a,b) for the non-rotating model, and yields the better estimate of both the LLJ height, and surface heat and momentum fluxes. Yet another difference can be seen between U_{WKB} and U_s: both profiles have the return flow around $z \approx 200$ m of similar amplitude, but this layer is thicker for the $K(z)$ case.

The sharper near-surface gradient and the lower LLJ height are also seen for the cross-slope wind component V, when $K(z)$ is employed, Fig. 3. There V_{num} still diffuses upwards but, as expected, its propagation is now limited to the height where the values of $K(z)$ approach zero ($z \approx 800$ m, Fig. 2). This leads us to the conclusion that the hypothesis of V influencing the polar vortex after sufficient time imposed by Stiperski et al. (2007) should be more relaxed in this more realistic case. There is another significant difference, i.e., the presence of a secondary bulge in V above the height of $K_{\max}$ at $z \approx 400$ or 500 m. As the integration time increases, this bulge strengthens and expands with height, nevertheless obeying the limitations imposed by $K(z)$. The bulge in $V(z,t)$ occurs because of two opposing effects. Both $V(z,t)$, namely V_{num} and V_{WKB}, try to diffuse upwards as in the 1st Stokes problem, which is nicely emulated in Stiperski et al. (2007). However, at progressively higher levels there is less and less $K(z)$ for mixing the V component upward. Hence, $V(z,t)$ finds less and less medium to diffuse through and starts to accumulate below $K(z) \to 0$ level (Fig. 3, black solid line). On the contrary, deep and non-decaying K supports the vertical diffusion of $V(z,t)$ (Fig. 3, grey solid line).

The overall behaviour of V_{num} is very well described with the new approximate WKB solution V_{WKB} from (18), only slightly overestimating the maximum amplitude. Similar behaviour of the analytical solution V_f has also been observed for the constant-K case in Stiperski et al. (2007). The detailed calculation presented here for $V(z,t)$ also explains the behaviour of the V component in Denby (1999), which was not commented there (see his Figure 2e and 5).

Additional remarks on how to estimate the input parameters for this Ekman–Prandtl model type with $K(z)$ can be found in Parmhed et al. (2004); Parmhed et al. (2005). The new analytical solutions $(U,V,\theta)_{\mathrm{WKB}}$, (16), (17) and (18) are not named "asymptotic", which usually holds for the WKB solutions, only because we weakly decoupled (2) so that V_{WKB} does not feed back to the original system (1)–(3). The numerical result shows, as also in Stiperski et al. (2007), that the V effect on the katabatic dynamics is negligible. However, the induced $V(z,t)$ affects the wind direction and the horizontal momentum flux.

4 Conclusions

A better understanding of katabatic flows is necessary for better treatment and parameterization of the coupling between the atmosphere and cool, inclined surfaces (e.g., King et al. 2001; Weng and Taylor 2003). The rotating Prandtl model (Stiperski et al. 2007), although providing the analytical tool for analyzing this coupling, does not hold for the real atmosphere due to the assumption of constant eddy diffusivity. In this work an attempt is made towards a more realistic description of the long-lived katabatic strongly stable ABL through the approach of Grisogono and Oerlemans (2001a,b). There, the asymptotic solutions for the Prandtl model with gradually varying $K(z)$, but without rotation, were obtained using the WKB method. The obtained solutions

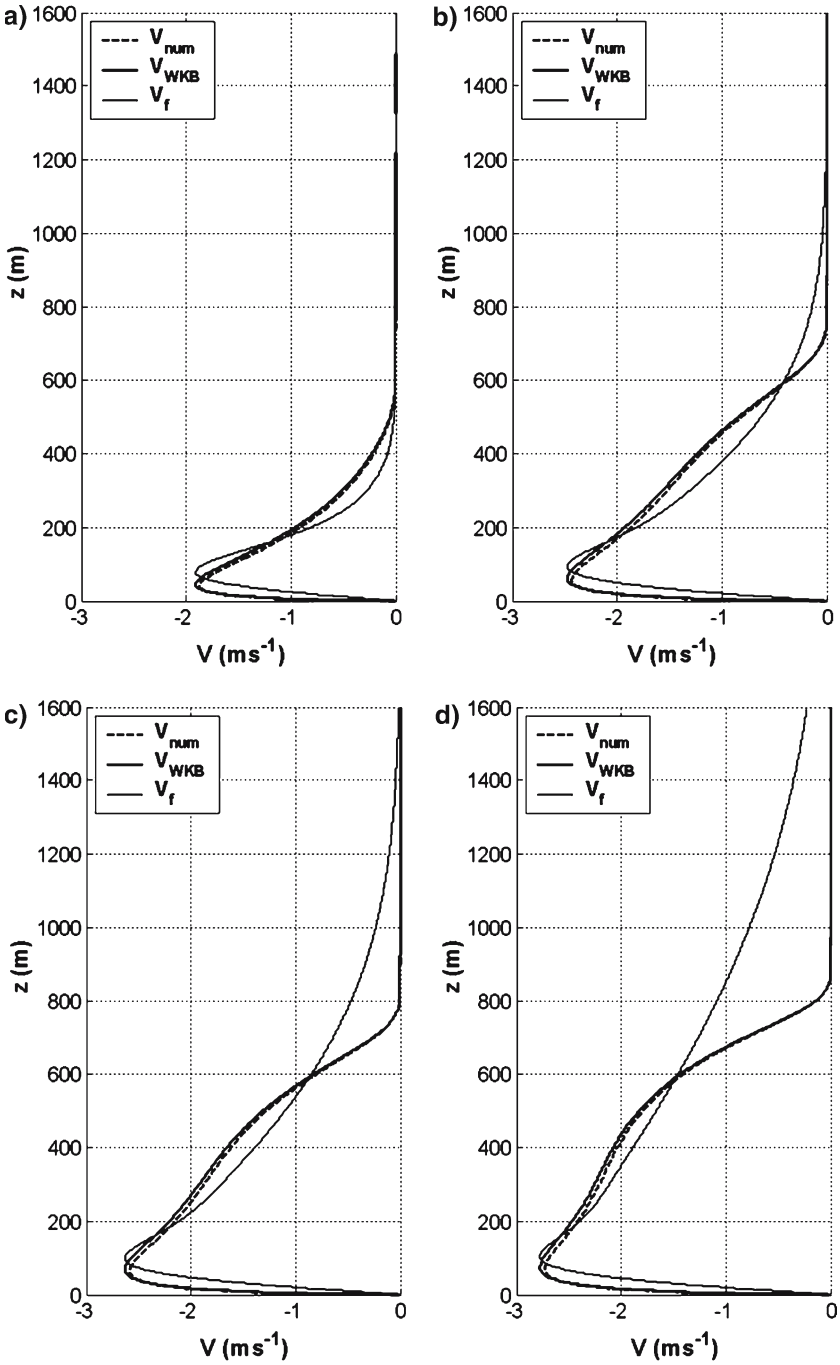

Fig. 3 The analytical (solid) and numerical (dashed) solutions for V at (**a**) $t = 2T$, (**b**) $t = 10T$, (**c**) $t = 20T$ and (**d**) $t = 50T$. The WKB solution V_{WKB} is in (18); the constant K solution, V_f, is given in (10). The rest as in Fig. 1

were verified against the results from the numerical model (Grisogono 2003), and independently against a dataset from Breidamerkurjokull, Iceland (Parmhed et al. 2004). Here, the analytical and numerical solutions for (U, V, θ) depending on (z, t) in the rotating katabatic flow are presented.

As expected, the overall change of the flow vector (U, V, θ) is structurally similar to the constant-K case (Stiperski et al. 2007). Both U and θ reach their steady-state profiles after the typical time scale for simple katabatic flows $T \approx 2\pi/(N \sin(\alpha))$, and V still diffuses upwards in time without a well-defined time scale. Contrary to the constant-K case, the upward propagation of $V(z, t)$ is now limited by the vertically decaying values of $K(z)$ above its maximum. As the result, the elevated bulge in the $V(z, t)$ profile is observed above the weak return flow in U. This feature indicates the trapping of the V momentum at the height where $K(z)$ approaches a zero value, whereas for the constant-K values the V momentum continuously propagates under diffusion in the vertical (Stiperski et al. 2007). For example, if there was pre-existing elevated turbulence, e.g., residual turbulent layer(s), then the katabatic effect could, in principle, still influence the polar vortex after sufficiently long duration of the flow during the polar night.

This study shows that the WKB method of zero-order may be successfully applied to find the approximate analytical solutions for all the model components. The new WKB solution is relatively simple to derive and calculate either by analytical or numerical evaluation of the integral expression (13). The proposed analytical solutions (16), (17) and (18) can be used for studying katabatic flows over long slopes. Together with the introduction of the varying eddy diffusivity profile, the proposed solutions give a more realistic description of sloped surface-flux parameterizations in climate models and data analysis.

Acknowledgements Danijel Belušić is thanked for his insightful comments that helped to improve the manuscript substantially. Constructive criticism from three anonymous reviewers is appreciated. Ivana Stiperski, Dale R. Durran and Peter A. Taylor are thanked for the many fruitful discussions. This study was supported by the Croatian Ministry of Science, Education and Sports under the projects "Numerical methods in geophysical models" (No. 037-1193086-2771, Dept. of Mathematics), and "BORA" (No. 119-1193086-1311, Dept. of Geophysics).

References

Bender CM, Orszag SA (1978) Advanced mathematical methods for scientists and engineers. Mc Graw-Hill, Inc., New York, 593 pp

Defant F (1949) Zur theorie der Hangwinde, nebst Bemerkungen zur Theorie der Bergund Talwinde. Arch Meteor Geophys Biokl Ser A1:421–450

Denby B (1999) Second-order modelling of turbulence in katabatic flows. Boundary-Layer Meteorol 92:67–100

Egger J (1990) Thermally forced flows: theory. In: Blumen W (ed) Atmospheric processes over complex terrain. American Meteorological Society, Boston, MA, pp 43–57

Gordon AL, Comiso JC (1988) Polynyas in the Southern Ocean. Sci Am 258(6):90–97

Grisogono B (1995) A generalized Ekman layer profile within gradually varying eddy diffusivities. Quart J Roy Meteorol Soc 121:445–453

Grisogono B, Oerlemans J (2001a) Katabatic flow: analytic solution for gradually varying eddy diffusivities. J Atmos Sci 58:3349–3354

Grisogono B, Oerlemans J (2001b) A theory for the estimation of surface fluxes in simple katabatic flows. Quart J Roy Meteorol Soc 127:2725–2739

Grisogono B, Oerlemans J (2002) Justifying the WKB approximation in the pure katabatic flows. Tellus 54A:453–463

Grisogono B (2003) Post-onset behaviour of the pure katabatic flow. Boundary-Layer Meteorol 107:157–175
King JC, Conneley WM, Derbyshire SH (2001) Sensitivity of modelled Antarctic climate to surface and boundary-layer flux parameterizations. Quart J Roy Meteorol Soc 127:779–794
Kundu PK, Cohen IM (2002) Fluid mechanics, 2nd ed. Academic Press, San Diego, Calif., London, 730 pp
Mahrt L (1982) Momentum balance of gravity flows. J Atmos Sci 39:2701–2711
Munro DS (1989) Surface roughness and bulk heat transfer on a glacier: comparison with eddy correlation. J Glaciol 35:343–348
Munro DS (2004) Revisiting bulk heat transfer on the Peyto glacier in light of the OG parameterization. J Glaciol 50:590–600
Munro DS, Davies JA (1978) On fitting the log-linear model to wind speed and temperature profiles over a melting glacier. Boundary-Layer Meteorol 15:423–437
Oerlemans J (1998) The atmospheric boundary layer over melting glaciers. In: Holtslag AAM, Duynkerke PG (eds) Clear and cloudy boundary layers. Royal Netherlands Academy of Arts and Sciences, Place, VNE 48, ISBN 90-6984-235-1: 129–153
Parish TR, Bromwich DH (1991) Continental-scale simulation of the Antarctic katabatic wind regime. J Climate 4:135–146
Parmhed O, Oerlemans J, Grisogono B (2004) Describing the surface fluxes in the katabatic flow on Breidamerkurjokull, Iceland. Quart J Roy Meteorol Soc 130:1137–1151
Parmhed O, Kos I, Grisogono B (2005) An improved Ekman layer approximation for smooth eddy diffusivity profiles. Boundary-Layer Meteorol 115:399–407
Renfrew IA, Anderson PS (2002) The surface climatology of an ordinary katabatic wind regime in Coats Land, Antarctica. Tellus 54A:463–484
Renfrew IA (2004) The dynamics of idealized katabatic flow over a moderate slope and ice shelf. Quart J Roy Meteorol Soc 130:1023–1045
Renfrew IA, Anderson PS (2006) Profiles of katabatic flow in summer and winter over coats land, Antarctica. Quart J Roy Meteorol Soc 132:779–882
Söderberg S, Parmhed O (2006) Numerical modelling of katabatic flow over a melting outflow glacier. Boundary-Layer Meteorol 120:509–534
Stiperski I, Kavčič I, Grisogono B, Durran DR (2007) Including Coriolis effects in the Prandtl model for katabatic flow. Quart J Roy Meteorol Soc 133:101–106
Van den Broeke MR, van Lipzig NPM, van Meijgaard E (2002) Momentum budget of the East-Antarctic atmospheric boundary layer: results of a regional climate model. J Atmos Sci 59:3117–3129
Weng W, Taylor PA (2003) On modelling the one-dimensional atmospheric boundary layer. Boundary-Layer Meteorol 107:371–400
Zilitinkevich S, Savijärvi H, Baklanov A, Grisogono B, Myrberg K (2006) Forthcoming meetings on planetary boundary-layer theory, modelling and applications. Boundary-Layer Meteorol 119:591–593